Advanced Materials Research *Online: 2012-09-28*
ISSN: 1662-8985, Vol. 565, pp 430-435
doi:10.4028/www.scientific.net/AMR.565.430

Micro-structuring on Cylindrical Inner Surface using Whirling Electrical Discharge Texturing

Vitchuda Lertphokanont[1,a], Takayuki Sato[1], Minoru Ota[1,b], Keishi Yamaguchi[1], and Kai Egashira[1]

[1] Kyoto Institute of technology, Matsugasaki, Sakyo-ku, Kyoto, Japan

[a] vitchuda.lert@gmail.com, [b] m-ota@mech.kit.ac.jp

Keywords: Micro-structuring, Electrical Discharge Texturing, Whirling phenomenon, Texture-area ratio, Crater.

Abstract. The authors developed Whirling Electrical Discharge Texturing (WEDT) in order to reduce friction coefficient of cylinder-shaped parts. In previous research, the authors verified fundamental characteristics of WEDT by observation of textured surface. It was found that a crater shape and texture-area ratio can be controlled by WEDT. The texture-area ratio depends on feed speed of tool electrode. In this research, crater depth, crater diameter, texture area ratio and total removal volume of craters were investigated to confirm characteristics of WEDT in detail. In addition, tungsten wire was used as a whirling shaft in order to improve stability of whirling phenomenon. Moreover, a textured surface was finished by lapping-film in order to remove protrusions around craters and reduce friction coefficient. As a result, it was verified that the texture-area ratio slightly increased with decreasing feed speed and it was confirmed that crater depth, crater diameter, and total removal volume of craters were also related to feed speed.

Introduction

Recently, energy problems become an international concern since world's fossil fuel reserves are limited. To find new energy resource is difficult, therefore energy problems can be solved by improving energy efficiency. For example in transport machinery, energy efficiency can be improved by decreasing surface roughness and friction coefficient [1,2]. In addition, tribological characteristics can be controlled by processing microstructures on a surface which is not only to decrease friction coefficient but also maintaining good lubricated condition [3,4]. Therefore, microstructure was studied to process on a sliding part of transport machininary [1,5]. In general, microstructures are processed by cutting or laser beam maching and so on. However, cutting is difficult to process on high hardness material surface and laser beam machining is difficult to process on inner surface of cylindrical part. Because, lots of bearing with high hardness material and small diameter are used in the transport machinary, an effective process is required. EDM is a manufacturing process which is able to process a high hardness material and small diameter parts. Thus, EDM has been selected in order to process microstructures. The authors developed Whirling Electrical Discharge Texturing (WEDT) for high efficient texturing technique on the component surface of transport machinery. In WEDT, tool electrode shaft was whirling along inside a cylinder with high speed. In addition, gap voltage with high frequency was applied to generate craters on surface with high efficiency [6]. Moreover, in order to reduce friction coefficient, textured surface with low surface roughness is also required on parts [7]. Therefore, finishing process with lapping-film is needed after texturing with WEDT.

Principle of WEDT

In this study, WEDT is used as a technique for texturing on cylindrical inner surface in order to process a microstructure which is expected to improve friction characteristics. WEDT method is combined Electrical Discharge Texturing (EDT) and whirling phenomenon. A schematic model of WEDT process principle is described in Fig. 1. When the gap voltage is applied to the tool electrode,

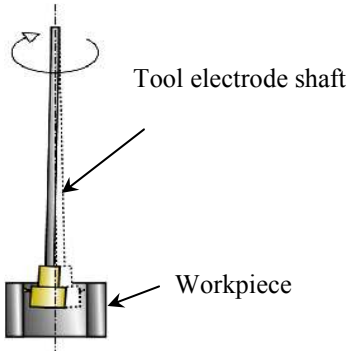

Fig. 1 Schematic model of WEDT process principle.

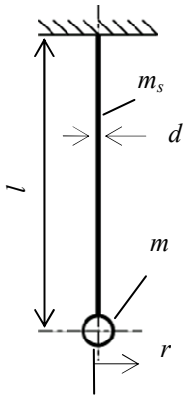

r	:	Displacement
ε	:	Degree of eccentricity
ω_0	:	Natural frequency
ω	:	Number of revolutions
l	:	Shaft length
m	:	Mass of the shaft
m_s	:	Mass of the electrode
d	:	Shaft diameter
E	:	Young's modulus
ζ	:	Damping ratio

Fig. 2 Cantilever model.

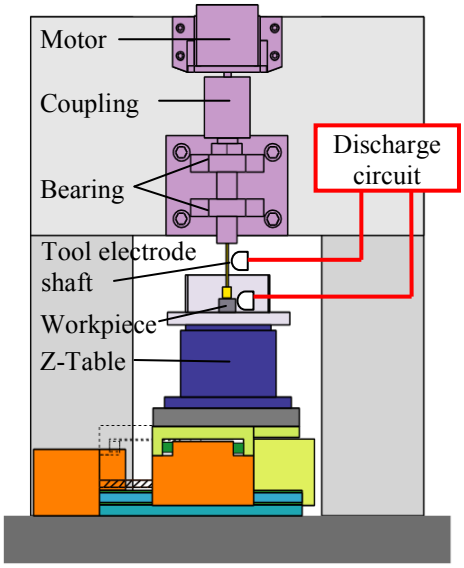

Fig. 3 Schematic diagram of WEDT equipment.

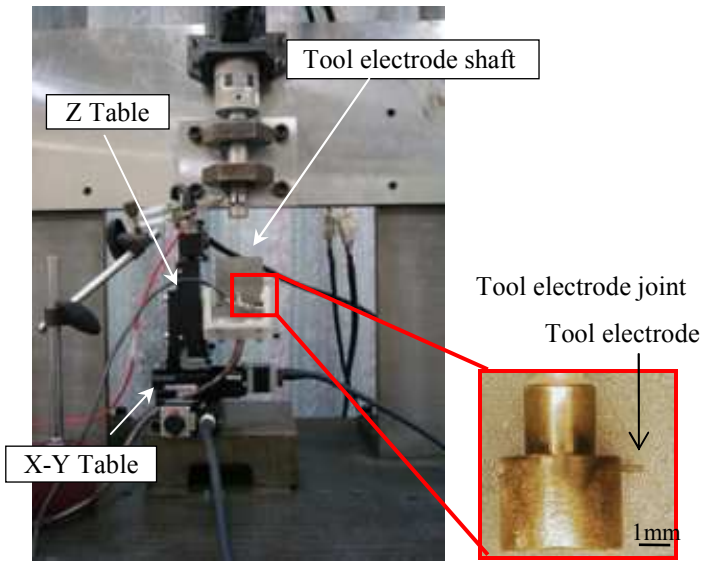

Fig. 4 Photograph of WEDT equipment.

the tool electrode shaft rotated with high speed, whirling phenomenon which is deflection of tip of tool electrode occurs. If the gap distance between the tool electrode and the workpiece is optimum value, discharge occurs and crater is generated on the workpiece surface. In WEDT, the shape of crater depends on the discharge current and pulse duration. In addition, texture-area ratio can be controlled according to the feed speed [6]. A horizontal displacement with rotating shaft is obtained by a cantilever model as shown in Fig. 2. Eq. 1 shows equation of the displacement and rotational speed and Eq. 2 shows equation of natural frequency of rotation.

$$r = \varepsilon \frac{\omega^2}{\sqrt{(\omega_0^2 - \omega^2)^2 + (2\zeta\omega)^2}} \tag{1}$$

$$\omega_0 = \sqrt{\frac{3\pi d^4 E}{64 l^3 (m + 0.23 m_s)}} \frac{60}{2\pi} \tag{2}$$

Experimental equipment

A schematic diagram of WEDT equipment is shown in Fig. 3. The whirling system consists of motor, coupling, bearing, and tool electrode shaft. The workpiece is fed in vertically by Z-table. Next, a photograph of WEDT equipment is shown in Fig. 4. The tool electrode was made of tungsten wire with 0.3 mm in diameter and 0.7 mm in length, which was inserted in the tool electrode joint. It is

assembled at the end of the whirling shaft. In addition, tungsten wire with 1 mm in diameter was used as whirling shaft in order to improve stabilization of whirling phenomenon. The workpiece was a cylindrical part of 7 mm in diameter and made of hardened carbon steel (S45C). The gap distance is adjusted by controlling the rotational speed of tool electrode shaft. Since, the deflection of tool electrode shaft is proportional to the rotational speed. So it can be controlled to get high rotational speed from whirling phenomenon.

WEDT experiment

Texture-area ratio was used as a parameter in order to compare the textured surface since the texture-area ratio is easy to measure by Scanning White Light Interferometer (NewView 7300, Zygo Corporation). The texture-area ratio can be calculated from crater-area divided by measuring area. From previous research, it was found that the texture-area ratio depends on feed speed [6]. As a result, the texture-area ratio was increased with decreasing feed speed. However, when the feed speed was less than 0.125 mm/s, the texture-area ratio was increased significantly. Therefore, this experiment was conducted in order to confirm the relationship between texture-area ratio and electrical conditions by WEDT equipment. Table 1 shows texturing experiment conditions. In order to obtain the optimum crater shape, experiment conditions was determined from a preliminary experiment of previous research. Fig. 5 shows SEM images of textured surface when feed speed was (a) 0.125 mm/s, (b) 0.09 mm/s, (c) 0.05 mm/s and (d) 0.02 mm/s with different discharge current (1) 4 A, (2) 10 A and (3) 15 A.

Table 1 Texturing experiment conditions

Power supply [V]	100
Pulse frequency [Hz]	1000
Pulse duration [μsec]	100
Rotational speed [min^{-1}]	2200
Feed speed [mm/sec]	0.125, 0.09, 0.05, 0.02
Discharge current [A]	4,10,15

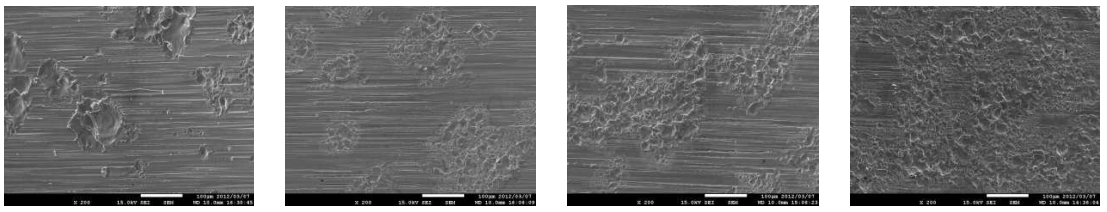

(a) (b) (c) (d) 100μm

(1) At discharge current 4 A.

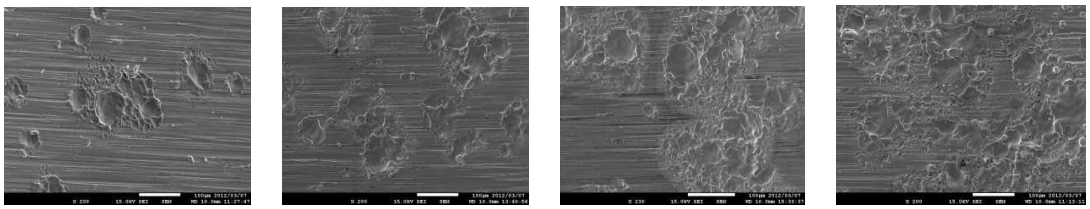

(a) (b) (c) (d) 100μm

(2) At discharge current 10 A.

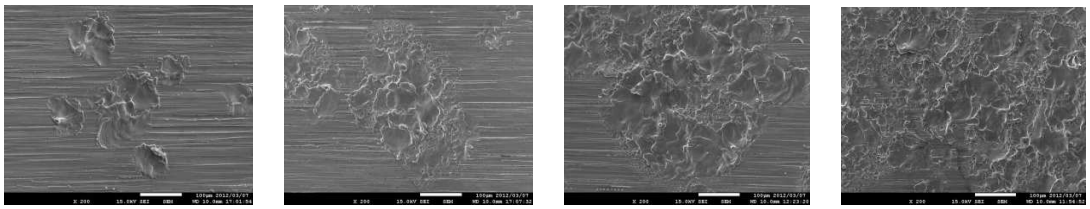

(a) (b) (c) (d) 100μm

(3) At discharge current 15 A.

Fig. 5 SEM images of textured surface

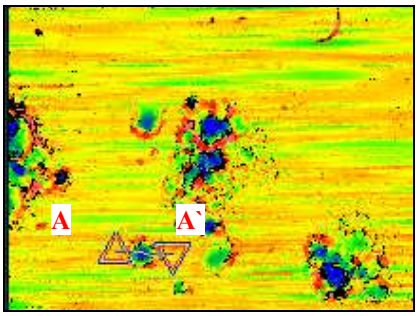

Fig. 6 2D image of textured surface obtained by ZYGO NewView 7300. (0.7 mm x 0.5

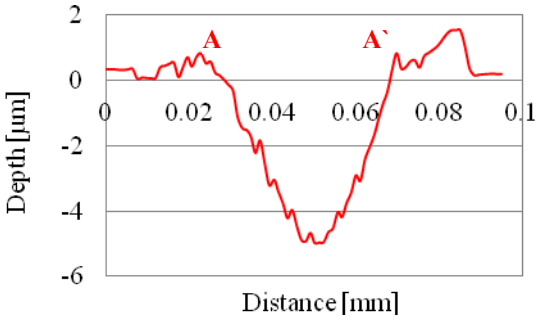

Fig. 7 Cross-sectional profile of crater.

Fig. 6 shows an example of 2D top view of the textured surface. Fig. 7 shows an example of cross-sectional profile of crater. The depth and diameter of each crater were measured through cross-sectional profile. From the result, the relationship between feed speed and texture-area ratio was obtained as shown in Fig. 8. At discharge current 10 A and 15 A, the texture-area ratio was moderately increased with decreasing feed speed. However, the texture-area ratio was significantly increased when feed speed was 0.02 mm/s and discharge current was 4 A. From surface observation after texturing, craters were overlapped at feed speed 0.02 mm/s because the distance between the tool electrode and protrusion formed by discharge became closer. Therefore discharge was easy to occur. In addition, the discharge that occurs on protrusion does not generate a normal crater, so lapping process was needed to remove the protrusion upon the textured surface. Fig. 9 shows relationship between feed speed and total removal volume of craters. It was clarified that total removal volume of craters depends on feed speed and discharge current. Fig. 10 shows relationship between feed speed and crater depth. The crater depth depends on feed speed and discharge current. At discharge current 4 A and 10 A, the crater depth was slightly increased with decreasing feed speed. However, crater depth was significantly increased at feed speed 0.02 mm/s and discharge current 10 A. Moreover, when discharge current was 15 A, crater depth became deeper than expected.

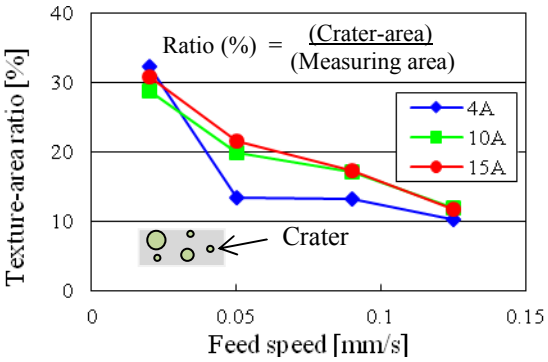

Fig. 8 Relationship between feed speed and texture-area ratio.

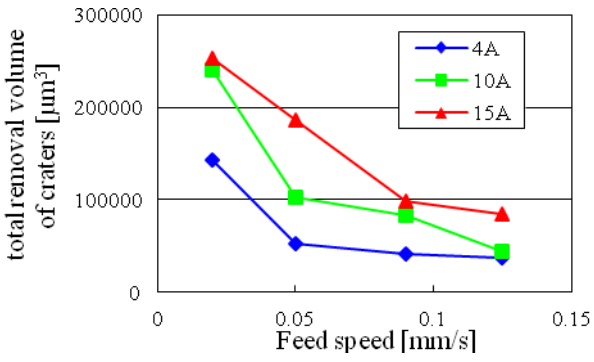

Fig. 9 Relationship between feed speed and total removal volume of craters.

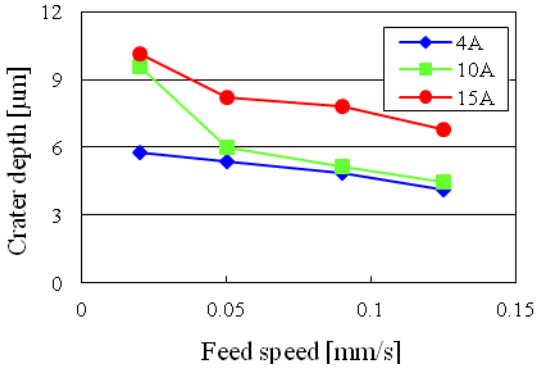

Fig. 10 Relationship between feed speed and crater depth.

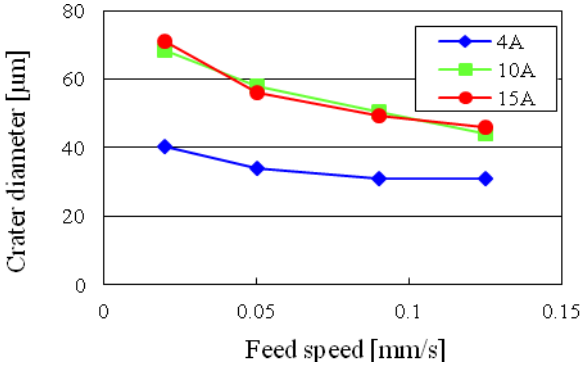

Fig. 11 Relationship between feed speed and crater diameter.

Fig. 11 shows relationship between feed speed and crater diameter. At discharge current 4 A, 10 A and 15 A, the crater diameter was slightly increased with decreasing feed speed. However, crater diameter at discharge current 15 A was not different from crater diameter at discharge current 10 A. From Fig. 11 at discharge current 15 A, it was thought that tool electrode length was not enough for discharge because tool electrode length has a limit. In this experiment, tool electrode feeding process was not considered. Thus during texturing process, tool electrode length was decreasing. When it was decreased, the gap distance became larger. Discharge energy was not enough for perfectly discharge, so the crater diameter at discharge current 15 A was less than expected. From Fig. 10 and Fig. 11, the value of crater depth and crater diameter in each condition was taken from the average of three samples of largest craters. Since discharge energy had influence on crater depth and crater diameter, the authors thought that crater depth and crater diameter were effect from discharge energy and it was distributed to crater depth and crater diameter. At discharge current 15 A, crater depth became deeper than expected and crater diameter was smaller than expected because of the discharge energy distribution. In this case, it was thought that discharge energy had more influence on crater depth than crater diameter.

Next, textured surface was finished by lapping-film in order to remove protrusions around crater that generated by discharge. In finishing process, aluminum oxide film 2 μm in mean grain size was attached to copper pipe of 6 mm in diameter and the pipe was chucked on the turning machine. Then it was rotated with 83 min^{-1} and pressed against the workpiece for finishing the textured surface with machining time 180 sec. Fig. 12 shows SEM images of textured surface after finishing process. Fig. 13 shows relationship between feed speed and texture-area ratio before and after finishing process at discharge current 4 A. Before finishing, when feed speed was 0.02 mm/s, the texture-area ratio was increased significantly. It was easy to generate crater at feed speed 0.02 mm/s due to a reduction of the gap distance and protrusions were generated around crater. After finishing, the texture-area ratio was slightly increased with decreasing feed speed. However, the texture-area ratio was decreased obviously at feed speed 0.02 mm/s. Because after finishing by lapping-film, protrusions were removed, consequently, texture-area ratio decreased significantly. Fig. 14 shows relationship between feed speed and total removal volume of craters before and after finishing at discharge current 4 A. Before finishing when feed speed was 0.02 mm/s, the total removal volume of craters was increased significantly. After finishing, it was slightly increased with decreasing feed speed. However, it was decreased obviously at feed speed 0.02 mm/s. Since after finishing by lapping-film, protrusions were removed, thus, the total removal volume of craters decreased significantly. Fig.15 shows relationship between feed speed and crater depth before and after finishing at discharge current 4 A. In finishing process, removal finishing allowance is not equal due to a difference in pressure. Thus, crater depth in each measuring point is different. After finishing, crater depth was decreased by 1 ~ 2 μm since part of textured surface which contained protrusions was removed. Fig.16 shows relationship between feed speed and crater diameter before and after finishing when discharge current was 4 A. Since, crater depth was decreased by 1 ~ 2 μm, crater diameter also decreased. It is thought that crater diameter was decreased in the different rate between feed speed 0.05 mm/s and 0.125 mm/s both before and after finishing by lapping-film because the measuring point on textured surface was different. It was expected that the measurement accuracy could be improved due to establish finishing method to remove protrusions.

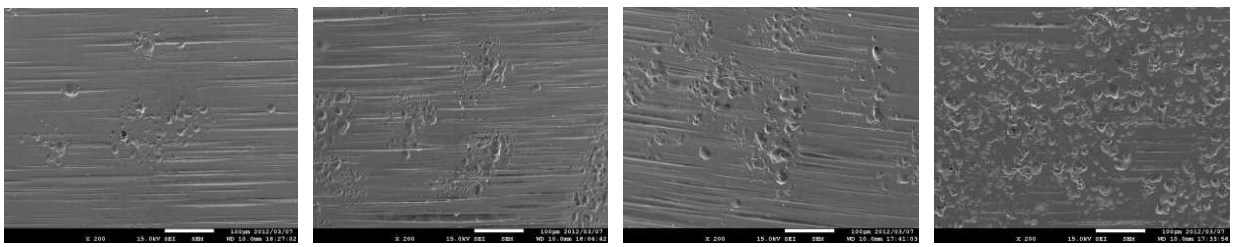

(a) 0.125mm/s (b) 0.09 mm/s (c) 0.05 mm/s (d) 0.02 mm/s ___ 100μm

Fig. 12 SEM images of textured surface after finishing at discharge current 4A.

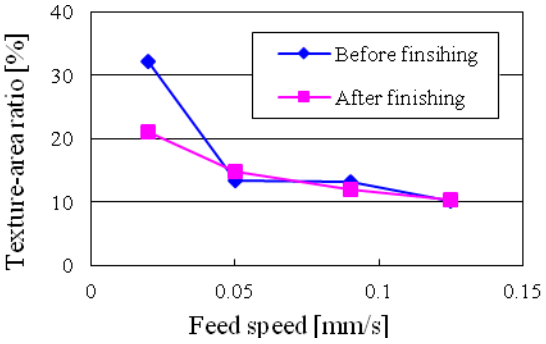

Fig. 13 Relationship between feed speed and texture-area ratio before and after finishing.

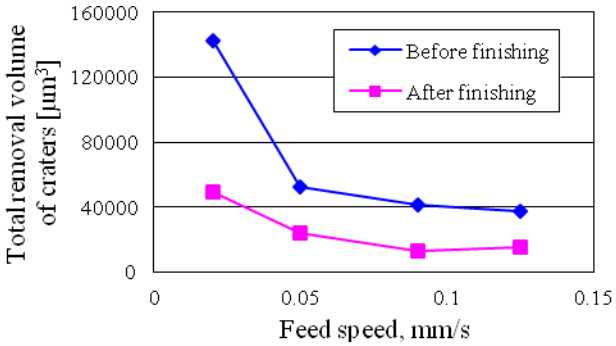

Fig. 14 Relationship between feed speed and total removal volume of craters before and after finishing.

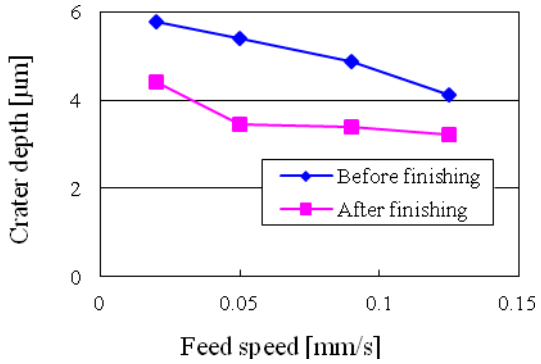

Fig. 15 Relationship between feed speed and crater depth before and after finishing.

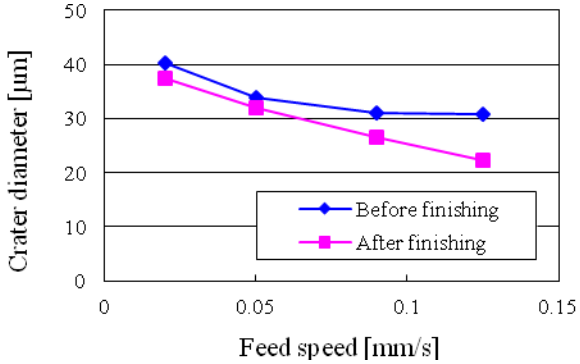

Fig. 16 Relationship between feed speed and crater diameter before and after finishing.

Conclusion

The following conclusions are obtained from the texturing experiment by WEDT method.

(1) From WEDT experiment, it was confirmed that the texture-area ratio depends on feed speed.

(2) It was found that crater shape and texture properties are able to control by feed speed and electrical conditions.

(3) After finishing with lapping-film, textured surface with low surface roughness were obtained. It was verified that the texture-area ratio slightly increased with decreasing feed speed. In addition, crater depth, crater diameter, and total removal volume of craters are also related to feed speed.

Reference

[1] M. Ota, T. Nakayama and K. Takasima: Novel Microsurface Machining Techniques for Powertrain Components, JSAE Annual Congress Proceedings, Vol.30, 6 (2006), pp. 11-14.

[2] N. Moronuki: Future trend of functional surfaces, Proceeding of the 4thManufacturing & Machine Tool Conference. Vol.02, 25 (2002), pp. 69-70 (In Japanese).

[3] M. Ota: Surface Finishing and Surface Function for Automotive Components, Journal of Society of Automotive Engineers of Japan, vol.62 (2008), pp.16-20 (In Japanese).

[4] C. J. Evans and J. B. Bryan: “Structured”, “Textured” or “Engineered” Surface, Annals of the CIRP, Vol.48, 2 (1999), pp.541-556.

[5] T. Hirayama: Improvement of hydrodynamic performances by surface texturing technologies, Journal of the Japan Society of Grinding Engineers, Vol.49, 6 (2005), pp. 308-31 (In Japanese).

[6] H. Yasui, V. Lertphokanont, M. Ota, T. Hamaoka and T. Yabunaka: Proceeding of the 6th International Conference on Micro Manufacturing, ICOMM, (2011), pp.83-89.

[7] D.Zhu, T.Nanbu, N. Ren, Y. Yasuda and Q.J. Wang: Model-based virtual surface texturing for concentrated conformal-contact lubrication, Vol.224 Part J (2010), pp.685-696.